IJST, Transactions of Electrical Engineering, Vol. 38, No. E2, pp 110-122
Printed in The Islamic Republic of Iran, 2014

GRADIENT DESCENT-BASED POWER ALLOCATION AND RECEIVERS' POSITIONING IN MIMO RADARS*

M. M. CHITGARHA, M. RADMARD**, M. NAZARI MAJD AND M. M. NAYEBI

Dept. of Electrical Engineering, Sharif University of Technology, Tehran, I. R. of Iran
Email: nayebi@sharif.ir

Abstract– In MIMO (Multiple Input Multiple Output) radar systems multiple antennas at transmit and receive sides are used to improve the detection performance. Two important parameters which have an effect on the coverage and performance of these systems are: the transmitters' power and the receivers' positions. In this paper, assuming the Rayleigh scatter model for the target, the probability of detection is obtained for a MIMO radar system, by designing the Neyman-Pearson detector. Then, an iterative procedure is proposed for appropriate positioning of the receive antennas', such that this probability of detection is improved. Finally, the transmitters' powers are determined based on the gradient descent algorithm.

Keywords– MIMO radar, Neyman-Pearson detector, antenna placement, power allocation, gradient descent

1. INTRODUCTION

There has been significant interest towards the use of MIMO in detection and radar applications recently. Generally, MIMO radars can be divided into two main categories: systems based on the use of widely separated antennas [1] and systems that use collocated antennas [2, 3].

The studies have shown that we can have enhanced detection performance (Diversity Gain) [4]–[7] and high resolution object localization (Spatial multiplexing Gain) [8] with a widely separated antennas scheme.

Also, it has been shown that antennas' positions can affect the performance of the MIMO system but little has been done on proper placement of such antennas. In [9], GDOP (Geometric Dilution of Precision) is introduced as a metric that expresses the effect of the positions of the transmitting and receiving elements on the relationship between the time delay estimation errors and the localization errors. There, plots of GDOP are served as a tool for identifying the relation between antennas' positions and the obtainable accuracy. Finally, through a number of examples, it is shown that a symmetrical deployment of sensors around the object to be localized, yields the lowest GDOP values. Therefore, [9] does not introduce a procedure to position the antennas, but provides a tool to study the performance from an accuracy point of view. In addition, GDOP can be viewed as a metric for localization accuracy. Similarly, in [10], [11], plots of GDOP are used to provide an indication of localization accuracy over the two-dimensional space.

In [12], after deriving the Cramer-Rao bound (CRB) of the velocity estimation, it is used to study the optimized configuration. In this case, the problem of appropriate antenna positioning is not addressed, but a tool is introduced to see the effect of antennas' positions on the velocity estimation of a target at a

*Received by the editors August 31, 2013; Accepted November 27, 2014.
**Corresponding author

specific position. It should be noted that in this paper, after designing the detector, a criterion based on the detection performance, and not just on the estimation bound or the localization accuracy is introduced.

In [13]–[15], a procedure is developed for placing the receive antennas in a MIMO passive coherent location (PCL) scheme, in which the noncooperative transmitters' positions and powers are not under control. In that scenario, the multiplication of the probabilities of missed detection of each receiver from each transmitter is used as a criterion.

Another obstacle in a MIMO system is the power allocation, i.e. determining each transmitter's power while keeping the overall power constant. In [16], the problem of waveform design for minimizing the mean square error (MMSE) in estimating the target's impulse response based on waterfilling is studied. This paper shows the effect of various power control strategies in the MMSE performance of the waveform design. It should be noted that in [16], only the case of extended targets with known positions is considered (in other words, it is not a power allocation strategy for covering an area). Also, it assumes that the extended target's impulse response is a Gaussian random vector. However, we will propose a method of determining the power of transmit elements using the Swerling model (Rayleigh scatter) for the targets, in order to cover a region of interest. Another note is that in the aforementioned paper, the effect of path loss is not considered at all, since all transmitters, similar to receivers, are at an equal distance from the target. However, here, we consider the allocation problem for widely separated antennas in order to cover a region of interest.

In [17], two resource allocation schemes for multiple detection systems are proposed. The first approach fully utilizes all available infrastructure in the localization process, i.e., all transmit and receive systems, while minimizing the total transmit energy. The power allocation among the transmit antennas is optimized such that a predefined estimation mean-square error (MSE) objective is met, while keeping the transmitted power at each station within an acceptable range. The second scheme minimizes the number of transmit and receive antennas employed in the estimation process by effectively choosing a subset of antennas such that the required MSE performance threshold is attained. In this paper, similarly, only the estimation is considered, while we need to detect the target first.

In [18], a scheme is proposed to adjust the power weights at the transmit antennas proportionally by taking into account the correlation and line-of-sight information present at the transmitters. Antennas that are correlated or perceive low line-of-sight reflectivity are allocated less power, so that the total available energy is spread across diversity branches and strong reflectors more, accordingly. It is shown that this work alleviates the performance of MIMO systems in the existence of correlation and Ricean scattering models. However, in this manuscript, we consider the Rayleigh scatter model for the targets (Swerling model) and do the power allocation without the assumption of having such information at the transmit side.

In sections 2 and 3, the problem is formulated and in section 4 efficient optimization algorithms are proposed for solving it. Section 5 provides simulation results to verify the performance of the proposed methods. Finally, section 6 concludes the paper.

2. SIGNAL MODEL

Assume that there are N_t transmit antennas, N_r receive antennas and a target to be detected. For simplification we have assumed that the target to be localized has no Doppler, although such assumption is not critical in our derivations. The reflection antenna is assumed to be omnidirectional, collecting signals arriving from all directions. At the receiver side, the signal is passed through a CAF processor to obtain the delays and Doppler frequencies of different echoes collected from the object to be detected. The threshold at the output of the CAF processor for declaring that an object is detected is determined by the desired false alarm rate (P_{fa}). In this case, the signal received at the n'th receive antenna is presented by

$$y_n(t) = \sum_{i=1}^{N_t} \frac{\alpha_i^n}{r_{1i} r_{2i}} \sqrt{\frac{E_i}{L}} s_i(t - \tau_{in}) + n(t) \tag{1}$$

where $s_i(t)$ is the i'th transmitted signal , r_{1i} and r_{2n} are the distance from the transmitter to the target and the distance from the target to the receiver, respectively, N_t is the number of transmitters, α_i^n is the cross-section gain of the object illuminated by the signal transmitted from the i'th transmitter and received by n'th receiver, E_i is the energy of the i'th transmitted signal, L is the channel loss, and τ_{in} denotes the delay from the transmitter to the target plus the delay from the target to the receiver. We assume the orthogonality of the transmitted signals, i.e.

$$\int_{-\infty}^{+\infty} s_k(t) s_{k'}^*(t+\tau) dt = \begin{cases} 1 & if\ k = k', \tau = 0 \\ 0 & otherwise \end{cases} \tag{2}$$

The bistatic delay of the echo from the i'th transmitter at the n'th receiver is:

$$\tau_i = \frac{r_{1i} + r_{2n}}{c} \tag{3}$$

In the general case, $n(t)$ has the white Gaussian distribution with zero mean and variance σ_n^2.

In the next part, we define the probability of missed detection (P_{miss}) as the probability that we miss all echoes of the desired object.

3. THE DETECTION PROBLEM

Now, we explore the probability of missed detection in this problem. The existence of a target in a specific bistatic range cell is a random process with unknown probability. Neyman-Pearson detector is used because priori probabilities are unknown. Consequently, we compare the likelihood ratio $L(\boldsymbol{y})$ with threshold η to derive the false alarm probability. So, by sampling the received signal presented in (1) at the n'th receiver, for a specific bistatic range cell, the hypotheses are as shown below:

$$\begin{cases} H_0 : \boldsymbol{y} = \boldsymbol{n} \\ H_1 : \boldsymbol{y} = \boldsymbol{n} + l\boldsymbol{s} \end{cases} \tag{4}$$

where vectors $\boldsymbol{y}$, $\boldsymbol{s}$ and $\boldsymbol{n}$ contain samples of received signal ($y_n(t)$), delayed signal ($s_i(t - \tau_{in})$) and noise ($n(t)$) with length m, respectively.

When there is no target, the signal at the receiver is white noise with variance of σ_n^2. However, if the target exists in the given bistatic range cell, it rejects the transmitted signal proportionally to its RCS. We assume that its RCS follows the Swerling I model (also called *Rayleigh scatter*). If σ^2 represents RCS, the distribution function of σ is:

$$f_\sigma(\sigma) = \frac{\sigma}{\sigma_t^2} e^{-\frac{\sigma^2}{2\sigma_t^2}} \tag{5}$$

where σ_t^2 is the RCS average value.

In equation (4) the coefficient l (the gain experienced by the signal from the transmitter to the receiver) is:

$$l = \frac{\sigma \nu}{r_{1i} r_{2n}} \tag{6}$$

where,

$$\nu = \sqrt{\frac{P_t G_t G_r I_p \lambda^2}{(4\pi)^3 L_c L_r}} \tag{7}$$

In (7), P_t is the transmitted power, G_t and G_r are the transmitting and receiving antenna gains respectively, I_p is the processing gain at the receiver, λ is the carrier wavelength, L_c is the scattering loss, and L_r is the receiver loss.

Without loss of generality, we assume that $||\boldsymbol{s}|| = 1$. The distribution function of l results from the distribution function of σ. Using (5) and (6) we have:

$$f_L(l) = \left(\frac{r_{1i}r_{2n}}{\nu\sigma_t}\right)^2 l e^{-\frac{1}{2}\left(\frac{r_{1i}r_{2n}}{\nu\sigma_t}\right)^2 l^2} \tag{8}$$

The problem of designing the Neyman-Pearson detector has been solved in [13] and the results are as follow.

The probability density function of the received signal in the H_0 and H_1 hypotheses are,

$$f_{\boldsymbol{Y}}(\boldsymbol{y}|H_0) = f_{\boldsymbol{N}}(\boldsymbol{y}) = \frac{1}{\left(\sqrt{2\pi}\sigma_n\right)^m} e^{-\frac{1}{2\sigma_n^2}\sum_{i=1}^m y_i^2} \tag{9}$$

$$f_{\boldsymbol{Y}}(\boldsymbol{y}|H_1) = \frac{a_0}{2a_1^2} e^{-\frac{1}{2\sigma_n^2}\sum_{i=1}^m y_i^2} \left(1 + \frac{a_2\sqrt{\pi}}{a_1} Q\left(-\frac{a_2}{a_1\sqrt{2}}\right) e^{\left(\frac{a_2}{2a_1}\right)^2}\right) \tag{10}$$

where,

$$Q(x) = \int_x^\infty \frac{1}{\sqrt{2\pi}} e^{-x'^2/2} dx' \tag{11}$$

$$a_0 = \frac{r_{1i}^2 r_{2n}^2}{\nu^2\sigma_t^2\left(\sqrt{2\pi}\sigma\right)^m} \quad , \quad a_1^2 = \frac{1}{2\sigma_n^2} + \frac{1}{2}\left(\frac{r_{1i}r_{2n}}{\nu\sigma_t}\right)^2 \quad , \quad a_2 = \frac{1}{\sigma_n^2}\sum_{i=1}^m y_i s_i \tag{12}$$

such that y_i and s_i are samples of $\boldsymbol{y}$ and $\boldsymbol{s}$ respectively. The Likelihood ratio is defined as:

$$L(\boldsymbol{y}) = \frac{f_{\boldsymbol{Y}}(\boldsymbol{y}|H_1)}{f_{\boldsymbol{Y}}(\boldsymbol{y}|H_0)} \tag{13}$$

By using (9), (10), (13) and simplifying the likelihood ratio we have

$$L(\boldsymbol{y}) = \frac{a_0\left(\sqrt{2\pi}\sigma_n\right)^m}{2a_1^2}\left(1 + \frac{a_2\sqrt{\pi}}{a_1} Q\left(-\frac{a_2}{a_1\sqrt{2}}\right) e^{\left(\frac{a_2}{2a_1}\right)^2}\right) \tag{14}$$

Using the fact that $L(\boldsymbol{y})$ is an increasing function of a_2, we can design the detector as

$$\sum_{i=1}^m y_i s_i \underset{H_0}{\overset{H_1}{\gtrless}} \eta \tag{15}$$

This equation shows that if we use the matched filter at the receiver, we have optimal efficiency in the detection of the target placed at a specific bistatic range cell. Subsequently, η must be determined to achieve the desired false alarm probability.

The false alarm probability is obtained as follows:

$$P_{fa} = Q\left(\frac{\eta}{\sigma_n}\right) \tag{16}$$

By substituting α instead of P_{fa}, the threshold value η is obtained:

$$\eta = \sigma_n Q^{-1}(\alpha) \tag{17}$$

and then, the detection probability is simplified as shown below:

$$P_d = \alpha + \frac{1}{\sqrt{2}\sigma_n b_1} e^{\left(\frac{b_2}{2b_1}\right)^2 - \sigma_n Q^{-1}(\alpha)\frac{b_2}{2}} Q\left(\frac{b_2}{b_1\sqrt{2}} - \sqrt{2}b_1\sigma_n Q^{-1}(\alpha)\right) \tag{18}$$

where,

$$b_1^2 = \frac{1}{2\sigma_n^2} + \frac{1}{2\sigma_1^2} = \frac{1}{2}\left(\frac{1}{\sigma_n^2} + \frac{r_{1i}^2 r_{2n}^2}{\nu^2\sigma_t^2}\right) \quad , \quad b_2 = \frac{\eta}{\sigma_1^2} = \frac{\eta r_{1i}^2 r_{2n}^2}{\nu^2\sigma_t^2} \tag{19}$$

The missed detection probability is also obtained as follows,

$$P_{miss} = 1 - P_d = 1 - \alpha - \frac{1}{\sqrt{2}\sigma_n b_1} e^{\left(\frac{b_2}{2b_1}\right)^2 - \sigma_n Q^{-1}(\alpha)\frac{b_2}{2}} Q\left(\frac{b_2}{b_1\sqrt{2}} - \sqrt{2} b_1 \sigma_n Q^{-1}(\alpha)\right) \tag{20}$$

Note that this is the probability of one pair of transmitter and receiver. The total probability of missed detection is the production of P_{miss}'s of each pair of transmitter and receiver. So, the total probability of missed detection can be written as

$$P_{miss} = \prod_{i=1}^{N_t} \prod_{j=1}^{N_r} P_{miss_{ij}} \tag{21}$$

where $P_{miss_{ij}}$ denotes the probability of missed detection of i's transmitter and j's receiver.

In Fig. 1, P_{miss} is (the total probability of missed detection) for two transmitters and one receiver is depicted. Table 1 shows the parameters of the scenario.

Table 1. Sample parameters

P_t	20 kW
λ	0.6 m
$G_r = G_t$	0 dB
F_n	7 dB
I_p	40 dB
$L_c L_r$	5 dB
σ_0^2	2.4 m^2
BW	6 MHz

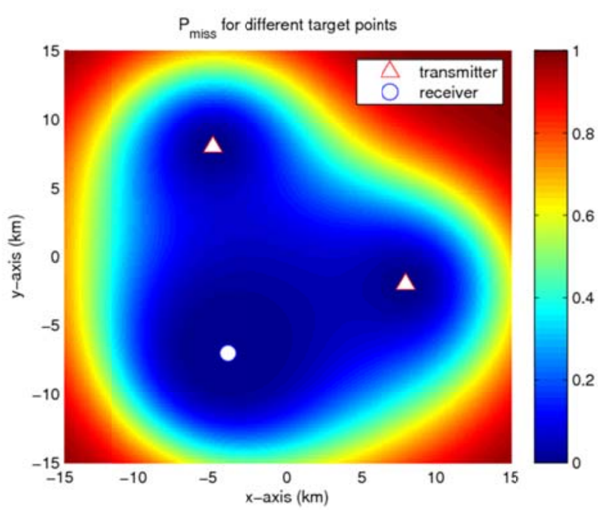

Fig. 1. P_{miss} for different target positions and sample antennas' positions

4. PROBABILITY OF DETECTION OPTIMIZATION

In this section, by changing receivers' positions and transmitters' powers, we optimize the probability of detection. The transmitters' positions are assumed to be constant.

In our scenarios, we define a priority function that represents the importance of detection of each location in our area of interest. In other words, the places with higher degree of importance (from the target's detection point of view) are assigned higher value in this function. Our priority function is formulated as in (22) and is shown in Fig. 2.

$$f_p(x,y) = e^{-0.05\sqrt{(x-4.15)^2+(y+7.35)^2}} \tag{22}$$

where (x, y) denotes the Cartesian coordinates of the location. Next, the receivers' positioning and then the power allocation algorithm is represented.

a) Receiver positioning

Here, we use the probability of missed detection in (21) as a criterion to find the optimum positions for placing the receivers.

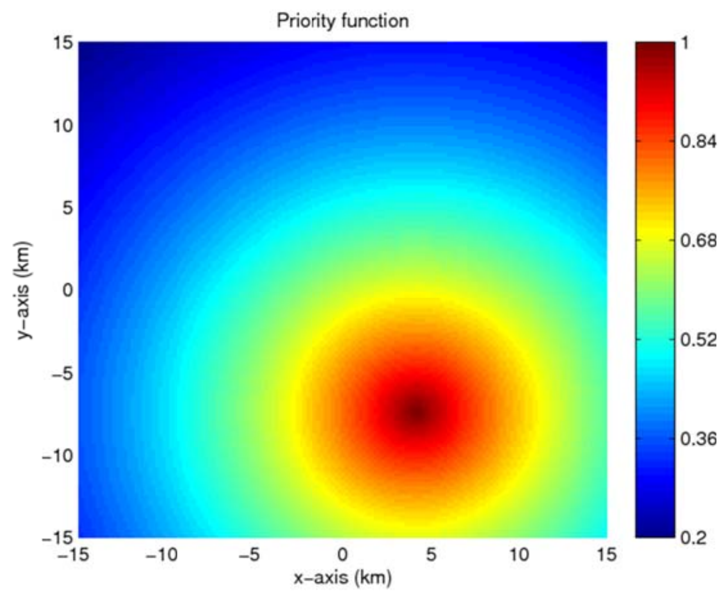

Fig. 2. Priority function

First, we weight the P_{miss} of each point proportional to the value of the priority function at that point. Next, we calculate the average value of the resulting total P_{miss} (for each set of receivers' positions) as the criterion. In other words, for each set of receivers' positions in the whole region, the average value of the weighted total P_{miss} of different target's positions in this region is computed. Then, over different sets of receivers' positions, the receivers' positions are chosen corresponding to the minimum of these average values, which results in better detection and less missed detection.

It should be noted that in [13] the same criterion (P_{miss}) is chosen. However, there, the receivers are positioned one after another, So that the coverage obtained by the second and third receivers has no effect on the position of the first receiver. Similarly, the coverage obtained by the third one has no effect on choosing the position of the second one. In other words, since the positions are chosen one by one, only the coverage of the already placed receivers is considered in the procedure of positioning a receiver. In this paper, as described, the receivers are positioned simultaneously. Clearly, this results in better receiver positioning and consequently better probability of detection.

b) Power allocation

In this part, assuming that the total transmit power is constant, we want to determine each transmitter's power in order to minimize the overall P_{miss} (which is a function of the transmit powers). To find the optimum powers, we use the gradient descent algorithm. In this algorithm, for minimizing the function $F(\boldsymbol{x})$, $\boldsymbol{x}_{n+1}$ is obtained from $\boldsymbol{x}_n$ as follows:

$$\boldsymbol{x}_{n+1} = \boldsymbol{x}_n - \mu \nabla F(\boldsymbol{x}_n) \qquad (23)$$

Our goal is to minimize the production of P_{miss}'s. So the partial derivative of this function relative to the power of each transmitter should be determined. Note that each $P_{miss_{ij}}$ is a function of the i'th transmitter power, P_i. Therefore, by taking the derivative of (20) with respect to P_i, we have:

$$\frac{\partial P_{miss_{ij}}}{\partial P_i} = e^{\left(\frac{b_2}{2b_1}\right)^2 - \frac{\sigma_n Q^{-1}(\alpha) b_2}{2}} \Big(-\frac{b_1'}{\sqrt{2}\sigma_n b_1^2} Q\big(\frac{b_2}{b_1\sqrt{2}} - \sqrt{2} b_1 \sigma_n Q^{-1}(\alpha)\big)$$
$$+ \frac{1}{\sqrt{2}\sigma_n b_1} Q\big(\frac{b_2}{b_1\sqrt{2}} - \sqrt{2} b_1 \sigma_n Q^{-1}(\alpha)\big)\big(\frac{b_2 b_2' b_1^2 - b_1 b_1' b_2^2}{2b_1^4} - \frac{\sigma_n Q^{-1}(\alpha) b_2'}{2}\big) \qquad (24)$$
$$+ \frac{1}{2\sqrt{\pi}\sigma_n b_1}\left(\frac{b_2' b_1 - b_1' b_2}{b_1^2\sqrt{2}} - \sqrt{2} b_1' \sigma_n Q^{-1}(\alpha)\right) e^{-\frac{\left(\frac{b_2}{b_1\sqrt{2}} - \sqrt{2} b_1 \sigma_n Q^{-1}(\alpha)\right)^2}{2}}$$

where

$$b_1' = \frac{\partial b_1}{\partial P_i} = -\frac{(4\pi)^3 r_1^2 r_2^2 L}{4P^2 G_t G_r I_p \lambda^2 \sigma_t^2 \sqrt{\frac{1}{2\sigma_n^2} + \frac{(4\pi)^3 r_1^2 r_2^2 L}{2P_i G_t G_r I_p \lambda^2 \sigma_t^2}}} \qquad (25)$$

$$b_2' = \frac{\partial b_2}{\partial P} = -\frac{\sigma_n Q^{-1}(\alpha)(4\pi)^3 r_1^2 r_2^2 L}{P_i^2 G_t G_r I_p \lambda^2 \sigma_t^2} \qquad (26)$$

By choosing appropriate μ, the algorithm converges to its minimum. In the following we study the algorithm's behavior.

Consider three transmitters, one receiver and one target placed in a square region as shown in Fig 3. The P_{miss}, with equal powers of transmitters is equal to 0.61.

After the power allocation strategy proposed here, this P_{miss} will decrease to 0.31. This sample scenario shows the satisfying performance of the algorithm.

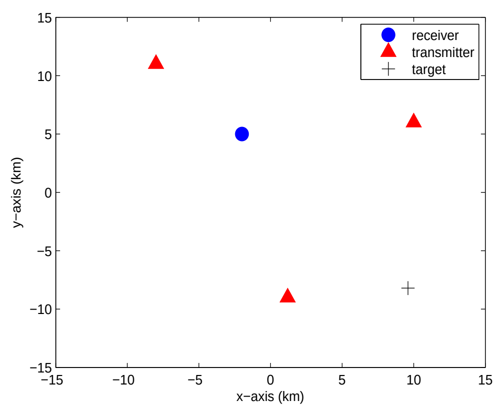

Fig. 3. A sample scenario with three transmitters, one receiver and a target

Now we change the target's position over the whole region and for each position, this algorithm is applied. Figures 4 and 5 show the probability of missed detection with equal powers and optimum powers, respectively. Note that in Fig. 5 for each target's position, the optimum powers are calculated and then P_{miss} using these powers is obtained. It can be seen that with applying this algorithm to allocate the transmit powers, better coverage is available.

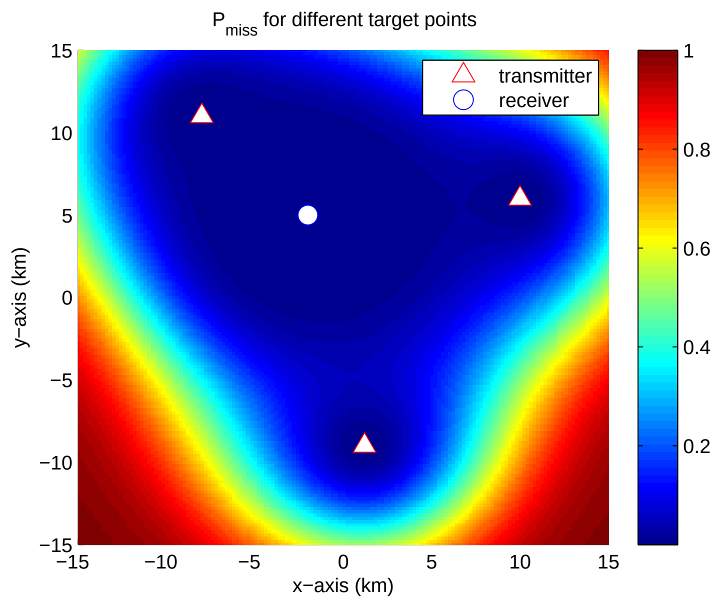

Fig. 4. P_{miss} with equal powers

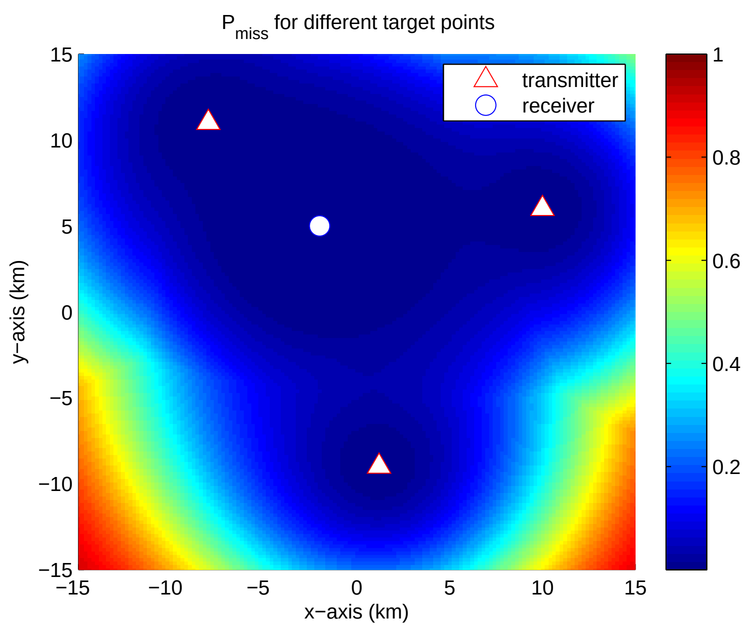

Fig. 5. P_{miss} with optimum powers

Now consider the second scenario shown in Fig. 6.

We change the target's position in the square plane and for each one, the optimum powers are calculated. The transmitters' powers for each target's position are shown in Figs. 7-9.

It can be seen that in the target's positions with high P_{miss} (e.g. in the corners of the plane), the algorithm causes a great increase in the power of the nearest transmitter and decrease in the others. On the other hand, in places with low P_{miss} (e.g. at the origin), equal powers are optimum. In fact, when dealing with high SNR (for all of the transmitters), if the total power is allocated to one transmitter, P_{miss} is proportional to inverse of P [1], and if we allocate total power uniformly to the transmitters, P_{miss} is proportional to inverse of $\left(\frac{P}{N_t}\right)^{N_t}$. Thus in high SNR, this function is exponentially decreased when powers are allocated equally. Also, it can be seen that for some target positions that are far from one transmitter, optimum power of this transmitter is zero. The reason of this fact is that in such places, the probability of missed detection using this transmitter is near one. So allocating power to this transmitter is less effective than allocating the power to a transmitter with lower probability of missed detection.

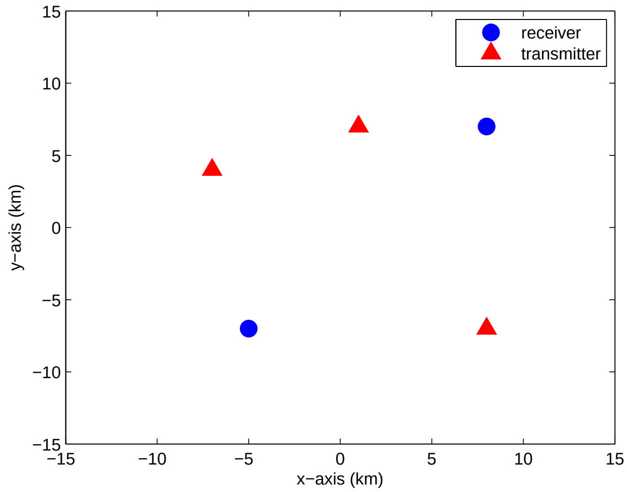

Fig. 6. Places of the transmitters and receivers

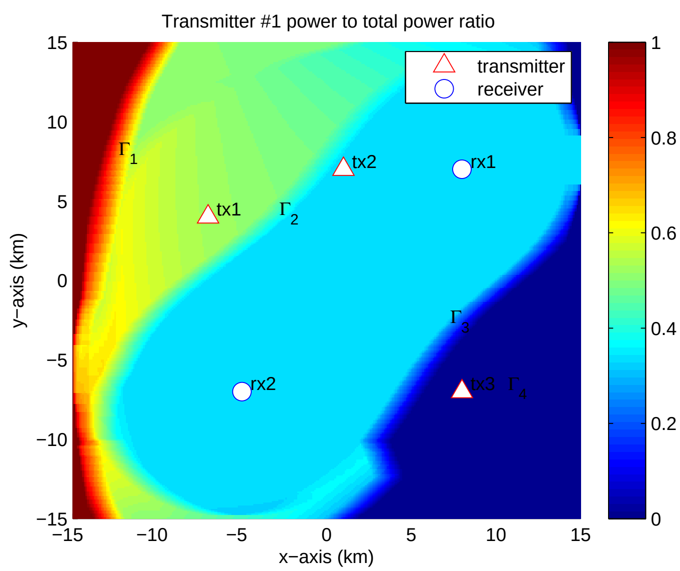

Fig. 7. The ratio of the first transmitter's optimum power to the total power

In Fig. 7, Γ_1 indicates the boundary above which the transmitters 2 and 3 have no sufficient SNR. Accordingly, no power is dedicated to these transmitters there and all is allocated to the transmitter 1. On the right side of this boundary, SNR of transmitter 2 is increased, but SNR of the transmitter 3 is still very low. Thus the total power is allocated to the transmitters 1 and 2. Also, because of the difference in SNR, power of the transmitter 1 is higher than power of the transmitter 2. In addition, power of the transmitter 3 is equal to zero until we reach the Γ_2 boundary. On the right side of this boundary, the total power is approximately allocated equally to all transmitters. In fact, in this region, SNR is so high that the optimum powers are approximately equal powers. So a MIMO radar system works properly in this region, resulting in advantages such as diversity, higher resolution. The same effect can be observed in other positions beyond the Γ_3 and Γ_4 boundaries.

The circumstances by which the optimum power of a transmitter is set to zero occurs when we deal with high probability of missed detection. By increasing the total power, positions with high probability of missed detection are decreased and thus the positions with zero power for such transmitter are reduced.

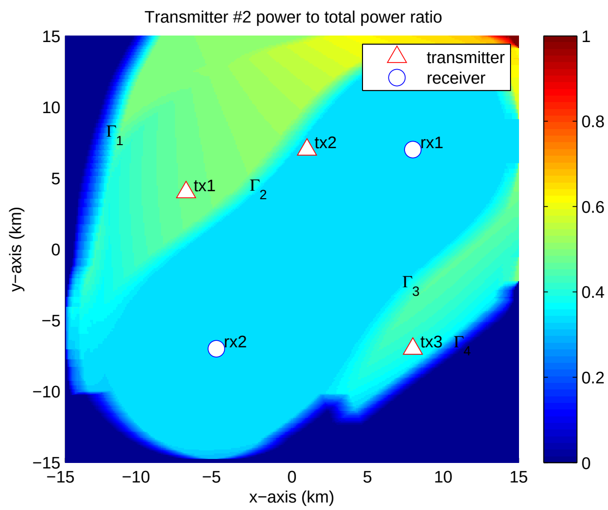

Fig. 8. The ratio of the second transmitter's optimum power to the total power

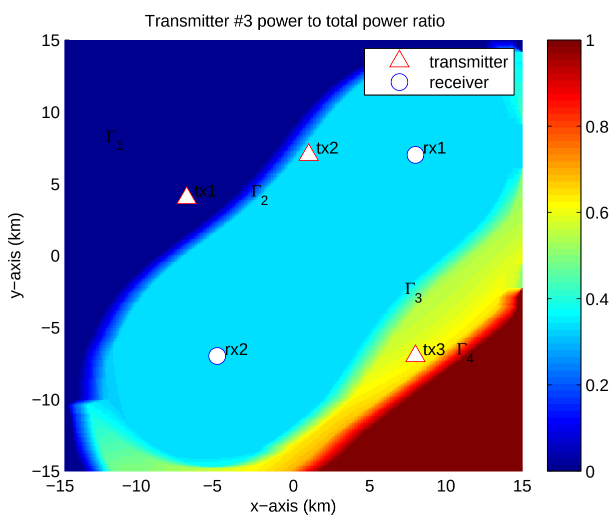

Fig. 9. The ratio of the third transmitter's optimum power to the total power

5. SIMULATIONS

In this section we use both receiver positioning and power allocation algorithms in one scenario to minimize P_{miss}. Transmitters' positions are assumed to be constant as shown in Fig. 10. Figure 11 shows P_{miss} with equal powers and arbitrary places of two receivers. In the following, the goal is to reach better coverage by assuming the priority function of (22).

First, assuming that the transmitters have equal powers, receiver positioning is applied and the positions of the two receivers are determined. Next, using the power allocation algorithm, the optimum powers for the three transmitters are obtained. Practically, it is not possible to vary the powers during the target's position's change. So the transmitters' powers are set to the average of their optimum powers weighted by the priority function of (22), while changing the target's position in the whole square region.

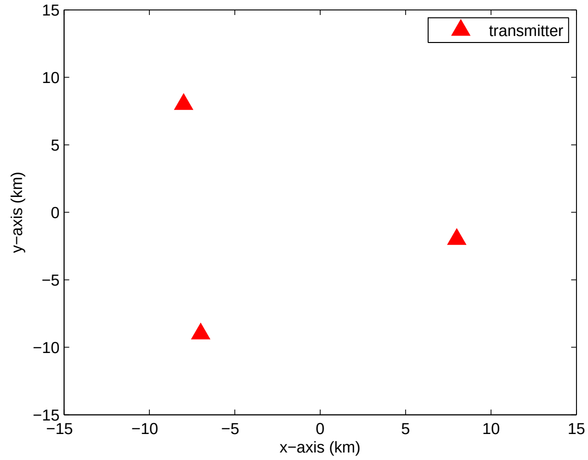

Fig. 10. Transmitters' positions

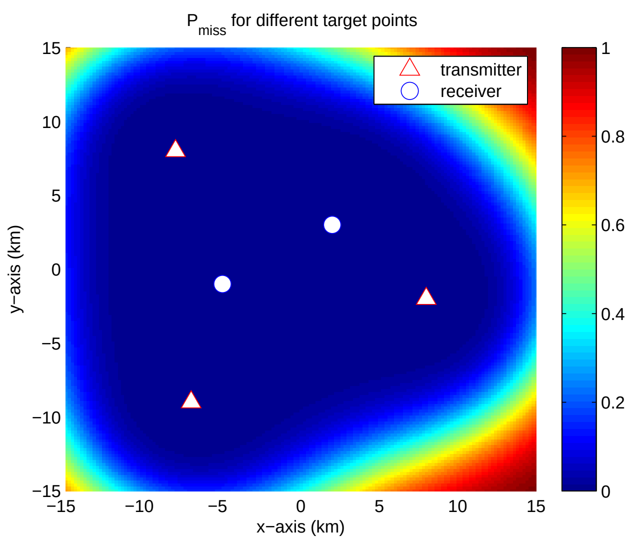

Fig. 11. P_{miss} with arbitrary receivers' places and equal powers

Now with these powers, receiver positioning is repeated and then power allocation algorithm is applied again. We continue this successive procedure until we reach a satisfying convergence. In this scenario, the convergence is obtained after five iterations. The receivers' positions and transmitters' powers of each iteration are shown in Tables 2, 3.

Table 2. Receivers' positions (km) in each iteration

Receiver	#1	#2
Iteration#1	[5.3 8.6]	[4.3 -9.5]
Iteration#2	[4.5 8.8]	[3.6 -9.2]
Iteration#3	[4.5 8.8]	[3.4 -9.2]
Iteration#4	[4.6 8.8]	[3.1 -9.2]
Iteration#5	[4.6 8.8]	[3.1 -9.2]

Table 3. Transmitters powers (kW) in each iteration

Transmitter	[-8 8] km	[-7 -9] km	[8 -2] km
Iteration#1	16.11	19.90	23.99
Iteration#2	15.94	19.46	24.59
Iteration#3	15.97	19.33	24.69
Iteration#4	16.10	19.10	24.80
Iteration#5	16.10	19.10	24.80

The final P_{miss} is shown in Fig. 12. It can be seen that using this method, a satisfying coverage is obtained.

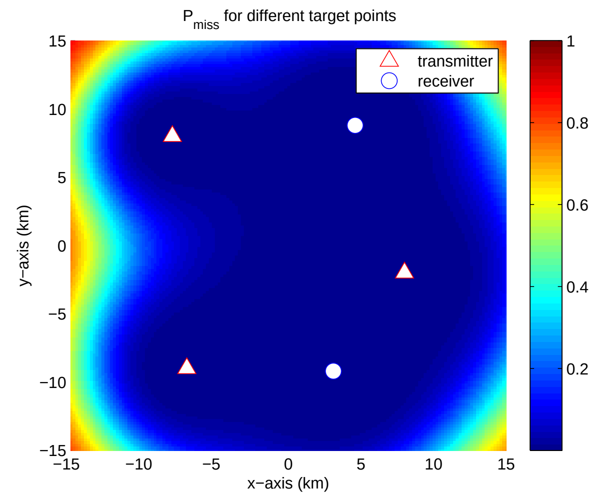

Fig. 12. P_{miss} after receivers' positioning and power allocation

6. CONCLUSION

In this paper, a method was introduced to receive antennas' positioning and one for determining the transmit powers in a MIMO radar system by maximizing the overall detection probability. The gradient descend algorithm was applied to choose the transmitters' powers. Also, a priority function was used to consider and model the importance of different places (e.g. from the surveillance point of view). Finally, both of these algorithms were used iteratively to reach a convergence for a good coverage from the detection probability viewpoint.

REFERENCES

1. Haimovich A. M., Blum R. S. & Cimini L. J. (2007). MIMO radar with widely separated antenna. *IEEE Signal Processing Magazine*, Vol. 25, 1, pp. 116–129.
2. Li, J. & Stoica, P. (2007). MIMO radar with colocated antennas. *IEEE Signal Processing Magazine*, Vol. 24, No 5, pp. 106–114.
3. M. Hatam, M., Sheikhi, A. & Masnadi-Shirazi M. A. (2011). A pulse-train MIMO radar based on theory of independent component analysis. *Iranian Journal of Science & Technology, Transactions of Electrical Engineering*, Vol. 35, No. E2, pp. 75-94.
4. Lehmann N. H., Fishler, E., Haimovich, A. M., Blum, R. S., Chizhik, D., Cimini, L. J. & Valenzuela, R. A. (2007). Evaluation of transmit diversity in MIMO-radar direction finding. *IEEE Transactions on Signal Processing*, Vol. 55, No. 5, pp. 2215–2225.
5. Fishler, E., Haimovich, A., Blum, R. S., Cimini, L. J., Chizhik, D. & Valenzuela, R. A. (2006). Spatial

diversity in radars-models and detection performance. *IEEE Transactions on Signal Processing*, Vol. 54, No. 3, 823–838.

6. Radmard, M., Karbasi, S. M. & Nayebi, M. M. (2013). Data fusion in MIMO DVB-T -based passive coherent location. *IEEE Transactions on Aerospace and Electronic Systems*, Vol. 49, No. 3, pp. 1725–1737.
7. Radmard, M., Chitgarha, M. M., Nazari Majd, M. & Nayebi, M. M. (2014). Antenna Placement and Power Allocation Optimization in MIMO Detection. *IEEE Transactions on Aerospace and Electronic Systems*, Vol. 50, No. 2, pp. 1468–1478.
8. Fishler, E., Haimovich, A., Blum, R. S., Cimini, L. J., Chizhik, D. & Valenzuela, R. A. (2004). MIMO radar: An idea whose time has come. *Proceedings of the IEEE Radar Conference*, pp. 71–78.
9. Godrich, H., Haimovich, A. M. & Blum, R. S. (2008). Cramer Rao bound on target localization estimation in MIMO radar systems. In *42nd Annual Conference on Information Sciences and Systems*, pp. 134–139.
10. Godrich, H., Haimovich, A. M. & Blum, R. S. (2010). Target localization accuracy gain in MIMO radar-based systems. *IEEE Transactions on Information Theory*, Vol. 56, No. 6, pp. 2783–2803.
11. Godrich, H., Haimovich, A. M. & Blum, R. S. (2009). Target localisation techniques and tools for multiple-input multiple-output radar. *IET Radar, Sonar & Navigation*, Vol. 3, No. 4, pp. 314–327.
12. He, Q., Blum, R. S., Godrich, H. & Haimovich, A. M. (2010). Target velocity estimation and antenna placement for MIMO radar with widely separated antennas. *IEEE Journal of Selected Topics in Signal Processing*, Vol. 4, No. 1, pp. 79–100.
13. Radmard, M., Khalaj, B. H., Chitgarha, M. M., Nazari Majd, M. & Nayebi, M. M. (2012). Receivers' Positioning in MIMO DVB-T Based Passive Coherent Location. *IET Radar*, *Sonar & Navigation*, Vol. 6, No. 7, pp. 603–610.
14. Nazari Majd, M., Chitgarha, M. M., Radmard, M. & Nayebi, M. M. (2012). Probability of missed detection as a criterion for receiver placement in MIMO PCL. In *IEEE Radar Conference (RADAR)*, pp. 924–927.
15. Chitgarha, M. M., Nazari Majd, M., Radmard, M. & Nayebi, M. M. (2012). Choosing the position of the receiver in a miso passive radar system. In *9th European Radar Conference (EuRAD)*, pp. 318–321.
16. Merline, A. & Thiruvengadam, S. J. (2011). Power allocation strategies for MIMO radar waveform design. *Iranian Journal of Electrical and Electronic Engineering*, Vol. 7, No. 2, pp. 106–111.
17. Godrich, H., Petropulu, A. & Poor, H. V. (2010). Resource allocation schemes for target localization in distributed multiple radar architectures. In *Proceedings of the European Signal Processing Conference*.
18. Akhtar, J. (2010). Energy allocation for correlated MIMO radar antennas with Ricean targets. In *11th International Radar Symposium (IRS)*, pp. 1–4.